# Supernova Remnants: Powerful agents of stars formation feedback. The case of IC 443

**P. Boumis[1], Zhi-Yu Zhang[2], I. Leonidaki[1] , E. Xilouris[1], S. Akras[3]**

[1] Institute for Astronomy, Astrophysics, Space Applications & Remote Sensing, National Observatory of Athens, Greece
2 IfA, University of Edinburgh (UK) / ESO
3 Observatorio do Valongo, Universidad Federal do Rio de Janeiro, Brazil

## Abstract

We present the results from our study on the effects of SNRs shocks on molecular clouds. We focused on the dense gas phase ($n>10^4$ cm$^{-3}$) from which the IMF emerges. We have used optical high-resolution echelle spectra as well as fully-sampled maps of $^{12}$CO J=1-0 and $^{13}$CO J=1-0. These sets of data along with published available 2MASS, Spitzer and 1.4GHz continuum maps are used as constraints on our radiative transfer codes in order to deduce the physical conditions for the dense gas in the shock-impacted areas of the molecular clouds.

## The case of Supernova Remnant IC 443

We have initiated a program (funded under the DeMoGas project*) to investigate the effects of these shocks much more closely, with a focus on the dense gas phase (n > $10^4$ cm$^{-3}$) from which the IMF emerges. Given the importance of SNRs in continuously injecting energy in the highly turbulent ISM of ULIRGs (e.g. there are ~50 SNRs in two disks of ~100 pc diameter in Arp 220), and that Sub-Millimeter Galaxies (SMGs) may be similarly compact starbursts (Swinbank et al. 2010), such a study is indeed timely. We have already acquired optical spectroscopic data from the 2.1-m SPM telescope in Mexico (see Figs. 2 & 3) as well as fully-sampled maps of $^{12}$CO J=1-0 and $^{13}$CO J=1-0 (Fig. 5). This unique set of data (e.g. optical velocities > 200 km/s where the molecular emission exists) along with publicly available 2MASS, Spitzer (Fig.4), and 1.4GHz continuum maps will be used as constraints on our radiative transfer codes in order to deduce the physical conditions of the dense gas in the shock-impacted areas of the molecular clouds.

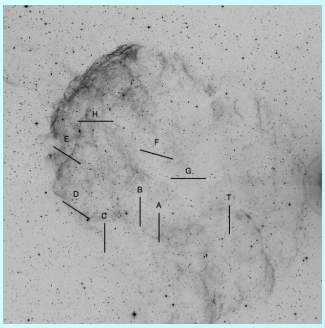


Fig. 1: Optical (POSS R) image of IC 443 where the slits of the observed echelle spectra can be seen.

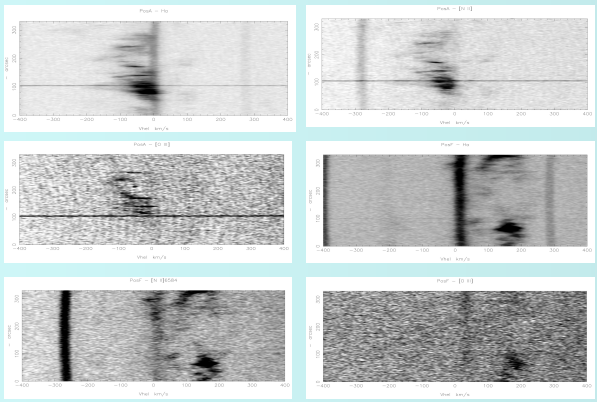

Fig.2: PV arrays showing longslit Hα, [N II]λ 6584 Å and [O III] 5007 Å SPM-MES spectra of IC 443 of slit positions A and F, aligned N–S and at P.A=64deg respectively, to show the nebular structure. North is to the top of the array. The velocity axis is heliocentric velocity, *V*hel, the y-axis is the slit length in arcsec. The vertical lines are airglow lines. .

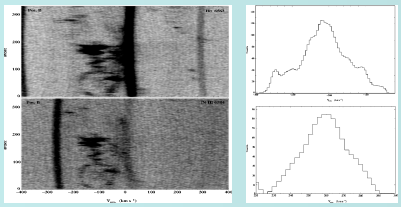

Fig.3: Left: PV arrays showing, Hα and [N II]λ 6584 Å SPM-MES spectra of IC 443 at slit position B, aligned N–S, to show the nebular structure. Right: The Hα line profiles from the highest speed knots, moving towards and away from the observer with velocities greater than 200 km/s.

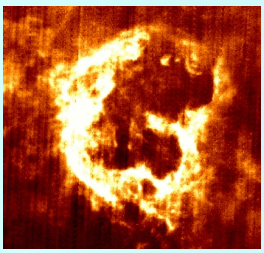

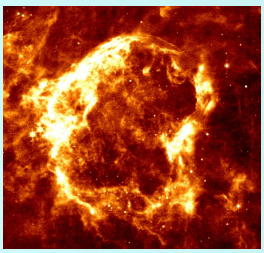

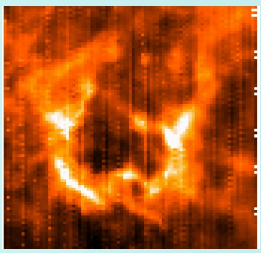

Fig. 4: Spitzer images at 24 μm, 70μm and 160μm where the IR emission of IC 443 can be seen.

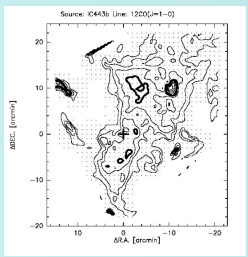


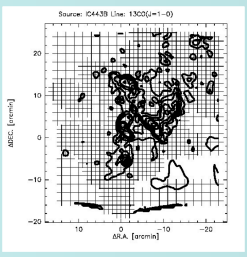


Fig.5: 12CO (left) and 13CO (right) J=1-0 map of IC 443.

| No | Target name G189.1+3.0 | R.A. (J2000) | Dec. (J2000) | exp. time (sec) | filter | slit (μm) | P.A. (o) | Highest knots Vhel (km/s) Hα | [N II] 6584 | [O III] |
|---|---|---|---|---|---|---|---|---|---|---|
| 1 | IC443 pos. A | 06:17:02.00 | 22:23:34.3 | 1800 | Hα+[N II],[O III] | 300 | 0 (NS) | -300, +200 | -300, +140 | -100, +100 |
| 2 | IC443 pos. B | 06:17:16.00 | 22:25:41.0 | 1800 | Hα+[N II] | 300 | 0 (NS) | -280, +260 | -220, +260 | - |
| 3 | IC443 pos. C | 06:17:42.21 | 22:21:41.0 | " | Hα+[N II] | " | 0 (NS) | -80, +40 | -80, +40 | - |
| 4 | IC443 pos. D | 06:18:03.40 | 22:26:17.0 | " | Hα+[N II],[O III] | " | 315 (NE-SW) | -80, +40 | -80, +40 | - |
| 5 | IC443 pos. E | 06:18:09.50 | 22:35:32.7 | " | Hα+[N II],[O III] | " | 315 (NE-SW) | -80, +120 | -80, +80 | -40, +40 |
| 6 | IC443 pos. F | 06:17:05.40 | 22:35:11.0 | " | Hα+[N II],[O III] | " | 64 | -200, +260 | -160, +260 | -160, +220 |
| 7 | IC443 pos. G | 06:16:41.62 | 22:31:41.0 | " | Hα+[N II] | " | 90 (EW) | -240, +300 | -220, +300 | - |
| 8 | IC443 pos. H | 06:17:46.50 | 22:41:32.5 | " | Hα+[N II],[O III] | " | 90 (EW) | -200, +160 | -200, +160 | -120, +60 |
| 9 | IC443 pos. T | 06:16:11.50 | 22:24:44.6 | " | Hα+[N II],[O III] | " | 0 (NS) | -150, +300 | -150, +200 | -80, +200 |

Table 1: summary of the optical observations and velocities of the SNR's knots in the areas where molecular emission exists.

## References

Arikawa et al. 1999, PASJ, 51, 7
Bolatto et al. 2003, ApJ, 595, 167
Sakamoto et al. 2008, ApJ, 684, 957
Seta et al. 1998, ApJ, 505, 286
Swinbank et al. 2010, Nature, 464, 733

## Acknowledgements

The project "DeMoGas" is implemented under the "ARISTEIA" action of the "Operational Programme Education and Lifelong Learning" and is co-funded by the European Social Fund (ESF) and National Resources.